

Kinetic Modeling of the Alkaline Decomposition and Cyanidation of Argentinian Plumbojarosite

Francisco Patiño,^{1*} Mizraim Uriel Flores,¹ Iván Alejandro Reyes,¹ Hernán Islas,¹ Martín Reyes,¹ and Guillermo Juárez²

¹ Área Académica de Ciencias de la Tierra y Materiales, Universidad Autónoma del Estado de Hidalgo, Carretera Pachuca-Tulancingo km. 4.5, C.P. 42184, Mineral de la Reforma, Hidalgo, México. franpac@terra.com.mx

² Centro de Investigaciones en Nuevos Materiales, Universidad Tecnológica de la Mixteca, Carretera a Acatlilma, km 2.5, C.P. 69000, Huajuapán de León, Oaxaca, México.

Received April 16th, 2013; Accepted July 23th, 2013

Abstract. The used sample was a solid plumbojarosite-argentinian jarosite-hydronium jarosite solution. The stoichiometry of the alkaline decomposition and cyanide reaction in alkaline medium were studied. Alkaline decomposition shows an induction period, as well as a conversion period. Results on the reaction order and activation energy are consistent with the spherical particle model with decreasing core and chemical control. Six partial models and three global models were developed in order to describe its basic behavior. In every case the models were validated and tested for a plumbojarosite conversion of $X = 0.75$

Key words: Plumbojarosite, stoichiometry, decomposition, alkaline, kinetics, models.

Resumen. La muestra utilizada es una solución sólida de plumbojarosita-arjentojarosita-hidroniojarosita. Se estudió la estequiometría de la reacción de descomposición y la de cianuración en medio alcalino. La descomposición alcalina muestra un periodo de inducción y un periodo de conversión. Los resultados de orden de reacción y energía de activación son consistentes con el modelo de núcleo decreciente y control químico. Se desarrollaron seis modelos parciales y tres modelos globales para describir su comportamiento básico. En todos los casos los modelos fueron validados y probados para una conversión de plumbojarosita de $X = 0.75$.

Palabras clave: Plumbojarosita, estequiometría, descomposición, alcalina, cinética, modelos.

Introduction

All the known members of the jarosite family are represented by the general formula: $M\text{Fe}_3(\text{SO}_4)_2(\text{OH})_6$, where M^+ is H_3O^+ , Na^+ , K^+ , Rb^+ , Ag^+ , NH_4^+ , Ti^+ , $\frac{1}{2}\text{Pb}^{2+}$, $\frac{1}{2}\text{Hg}^{2+}$ [1]. When one of these cations takes the place of M^+ , jarosite type compounds are formed. If the jarosite forms in nature, it receives a mineral name, while if it is obtained in the laboratory it receives a chemical name. When in nature $\frac{1}{2}\text{Pb}^{2+}$ substitutes M^+ , the formed mineral is given the name plumbojarosite; when that substitution is done through a synthesis procedure, it receives the chemical name lead jarosite. Plumbojarosite is a mineral that forms in acid media rich in sulfates, including zones of sulfur-type ore deposits that have undergone erosion, as well as acid rock drainage or acid mine drainage, and it usually forms around galena [2]. Lead jarosite is formed in the leaching circuits of zinc, and in pressure oxidation leaching processes of lead sulfide concentrates with associated silver [3].

Studies on the characterization of lead jarosite synthesized at 97 °C have suggested that all of the products contain H_3O^+ , Pb and Ag at different amounts according to the synthesis conditions. It is a solid ternary solution consisting of lead jarosite-hydronium jarosite-silver jarosite [3]. It is interesting to cite the lead jarosite structural model developed by Hendricks [4]: $\text{PbFe}_6(\text{SO}_4)_4(\text{OH})_{12}$ with $a = 7 \text{ \AA}$ and $c = 34 \text{ \AA}$; where Pb^{2+} takes up only half of the sites that are normally taken by Ag^+ cations. Therefore, part of the Pb^{2+} in the plumbojarosite can be replaced by 2 Ag^+ , but at some point the axis $c = 34 \text{ \AA}$

breaks, resulting in axis $c = 17 \text{ \AA}$, which is typical of argentinian jarosite.

The stability order of jarosites in function of iron precipitation degree is $\text{K} > \text{Ag} > \text{Rb} > \text{NH}_4 > \text{Na} > \text{Pb}$ [5, 6], while the stability order of jarosites in NaOH medium in function of their activation energy is $\text{Pb} > \text{Na} > \text{Rb} > \text{NH}_4 > \text{K} > \text{Ag}$ [7-12]. Jarosite residuals from the industry of lead and zinc usually contain silver, so through studies have been carried out on the alkaline cyanidation of these compounds [7-12]. It has also been found that these compounds incorporate arsenic in their lattice as AsO_4 in a partial substitution of SO_4 , making jarosites appealing from an economic [3, 13] and environmental point of view [14, 15, 16]. Because of the importance of plumbojarosite as an effective silver collector, Dutrizac *et al.* [17, 18, 19] conducted through studies on the incorporation of silver in the lattice of jarosite type compounds, both in sulfate and chloride media, with the aim of preventing the loss of silver in those compounds during their precipitation in the hydrometallurgical circuits of zinc and lead.

Patiño *et al.* [20, 21] studied the kinetics of the alkaline decomposition and cyanidation of argentinian plumbojarosite with the aim of establishing the stoichiometry of the reactions and the dependences on concentration of $\text{Ca}(\text{OH})_2$, NaOH and NaCN, as well as on temperature and particle size. However, those studies did not establish the partial and total kinetic expressions for the induction and progressive conversion periods. For this reason, this paper presents a comprehensive study on the kinetic modeling of the decomposition and cyanidation in

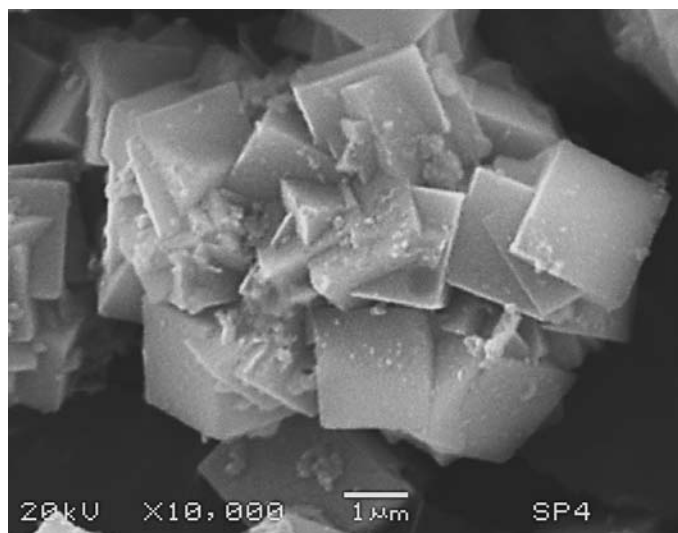


Fig. 1. Detailed image of a particle made of rhombohedral crystals of argentinean lead jarosite. SEM.

alkaline media of argentinean lead jarosite, validating each of the kinetic expressions established in this study.

Results and discussion

Nature of the reaction

Fig. 2 shows that the alkaline decomposition and cyanidation of argentinean lead jarosite presented an induction period (θ), during which the yellow color of the jarosite showed no changes, and the concentration of sulfate and silver ions remained at trace levels in the solution. This generally indicates that the decomposition and cyanidation reaction have not started. The end of the induction period was recognizable for a change in the superficial color of the solid, which went from yellow to

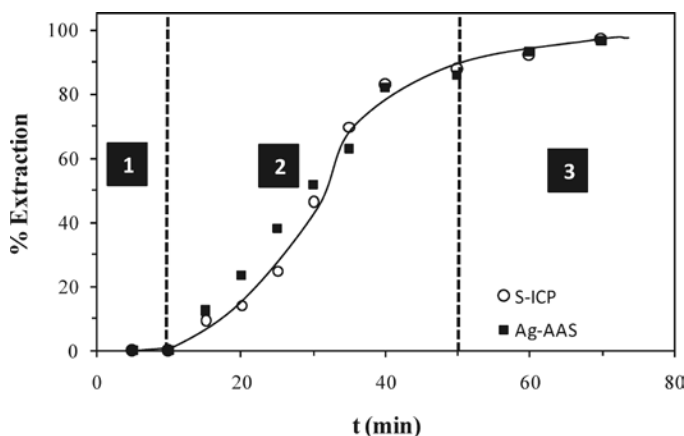
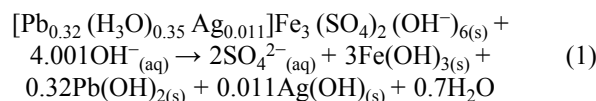
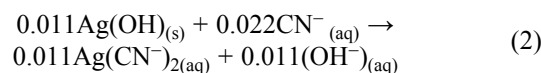


Fig. 2. Argentinean lead jarosite decomposition curve in $\text{Ca}(\text{OH})_2$ medium: pH 11.20, 40 °C. (1) Induction period, (2) progressive conversion period and (3) stabilization zone.

reddish. At the same time, the level of sulfate and silver ions in the solution increased progressively (Fig. 2) (as the reflection peaks of the argentinean lead jarosite decreased until disappearing (Fig. 3). The stabilization of the concentration of sulfate and silver ions (Fig. 2) indicated that the decomposition and cyanidation reaction had finished. According to this, the alkaline decomposition process can be represented by:



The solids resulting from the decomposition are made of a gel of amorphous iron, lead and silver hydroxides, as it occurs with the alkaline decomposition of other argentinean jarosites, such as sodium jarosite, rubidium jarosite, potassium jarosite and ammonium jarosite [8, 9, 11, 23]. Silver in the decomposition gel was solubilized by the cyanide ion. Therefore, the alkaline decomposition and cyanidation of argentinean lead jarosite can be described through two serial stages: first, a decomposition stage that controlled the overall process (Eq. 1), followed by a fast stage of complexation of $\text{Ag}(\text{OH})_{(s)}$, as expressed by the following equation:



The SEM examination of polished thin sections of partially decomposed argentinean lead jarosite proved to be difficult given the extremely small size of the jarosite crystals. However, EDS analysis (Fig. 4) is consistent with the formation of a reaction front. The spectrum of decomposed areas reveals the elimination of the sulfate ion, as well as the incorporation of the

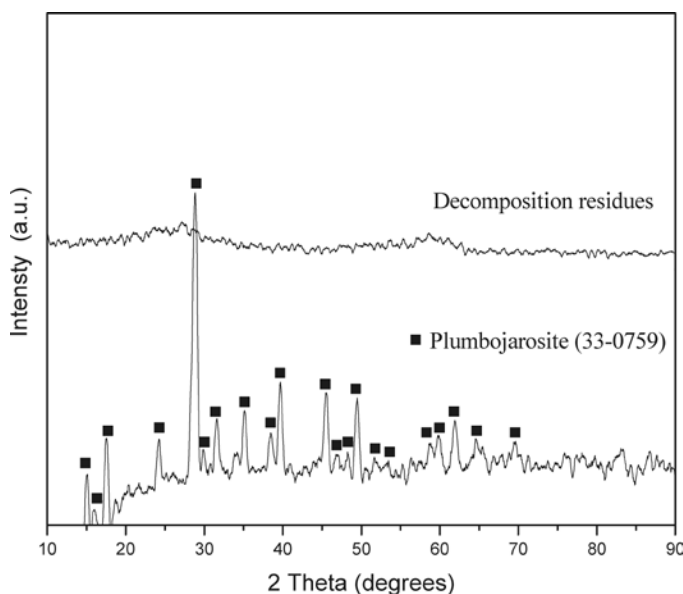


Fig. 3. Diffractogram of the solids resulting from the alkaline decomposition of argentinean lead jarosite in $\text{Ca}(\text{OH})_2$ medium: pH 11.20, 40 °C, 0-60 minutes.

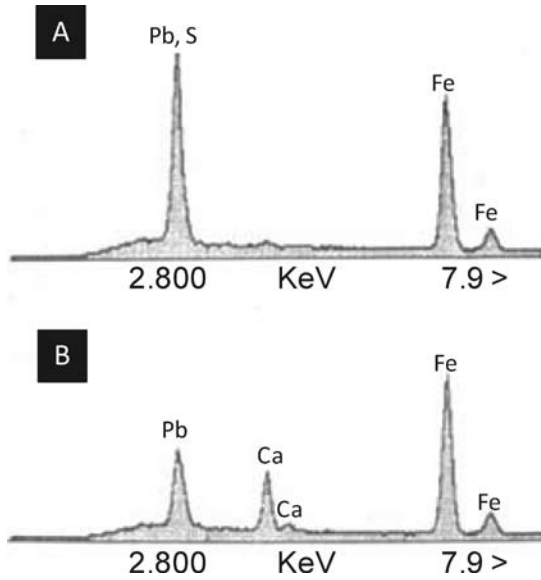


Fig. 4. EDS spectrum: a) unreacted internal area of argentian lead jarosite, b) decomposed outer rim (NaOH, pH 11.20, 40 °C).

calcium ion, which indicates that the decomposition products are porous enough to allow for the diffusion of ions in aqueous phase. Accordingly, the results of the alkaline decomposition and cyanidation of argentian lead jarosite are consistent with the spherical particle model with decreasing core and chemical control. This is confirmed in Fig. 5, where it can be noticed that the experimental data in Fig. 2 fairly match the mentioned model, which is expressed as [24, 25, 26]:

$$1 - (1 - X)^{1/3} = k_{\text{exp}} t \quad (3)$$

In which

$$k_{\text{exp}} = \frac{V_M K_q C_A^n}{r_0} \quad (4)$$

Where k_{exp} = experimental rate constant; X = reacted mole fraction; V_M = molar volume of the solid; K_q = chemical constant; C_A = reactant concentration; r_0 = initial radius and n = reaction order.

Modeling

Alkaline decomposition and cyanidation of argentian lead jarosite

Tables 1, 2 and 3 summarize the experimental results, in which the induction period (θ) and experimental rate constant (k_{exp}) are present in a wide range of experimental conditions, such as NaOH, $\text{Ca}(\text{OH})_2$, NaCN, temperature and particle size. pH was constantly adjusted during the whole reaction, and the concentration of OH ions was calculated according to the ionization constant of water at the working temperature of each experiment, as previously mentioned in the experimental section [22].

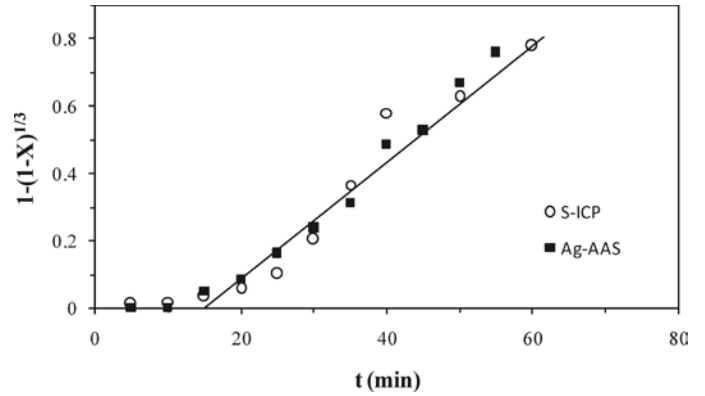


Fig. 5. Representation of the spherical particle model with decreasing core and chemical control for the data in Fig. 2.

Induction period

For the induction period of the decomposition of argentian lead jarosite in $\text{Ca}(\text{OH})_2$ medium with $[\text{OH}^-] > 3.39 \times 10^{-4} \text{ mol L}^{-1}$, a reaction order of $n = 0.1$ and an activation energy of $E_a = 68.56 \text{ kJ mol}^{-1}$ were obtained. In NaOH medium with $[\text{OH}^-] > 6.68 \times 10^{-3} \text{ mol L}^{-1}$, a reaction order of $n = 1.19$ and an activation energy of $E_a = 66.38 \text{ kJ mol}^{-1}$ were obtained. In the case of the cyanidation for $[\text{CN}^-] > 1.02 \times 10^{-2} \text{ mol L}^{-1}$, a reaction order of $n = 0$ and an activation energy of $E_a = 167.78 \text{ kJ mol}^{-1}$ were obtained. According to these results, the induction period for $\text{Ca}(\text{OH})_2$ is defined by the following expressions:

For $[\text{OH}^-] > 3.39 \times 10^{-4} \text{ mol L}^{-1}$

$$1/\theta = \frac{1}{(r_0 v_M)} \cdot [\text{OH}^-]^{0.1} \cdot 1.21 \times 10^9 \cdot e^{-68,568/RT} \quad (5)$$

For the induction period in NaOH medium with $[\text{OH}^-] > 6.68 \times 10^{-3}$, the following expression was obtained:

$$1/\theta = \frac{1}{(r_0 v_M)} \cdot [\text{OH}^-]^{1.19} \cdot 1.25 \times 10^{11} \cdot e^{-66,382/RT} \quad (6)$$

For the cyanidation with $[\text{CN}^-] > 1.02 \times 10^{-2}$, the following expression was obtained:

$$1/\theta = \frac{1}{(r_0 v_M)} \cdot [\text{CN}^-]^0 \cdot 4.22 \times 10^{26} \cdot e^{-167,780/RT} \quad (7)$$

Progressive conversion period

Regarding the progressive conversion period of the argentian lead jarosite decomposition in $\text{Ca}(\text{OH})_2$ medium with $[\text{OH}^-] > 3.39 \times 10^{-4} \text{ mol L}^{-1}$, a reaction order of $n = 0.5$ was obtained. The activation energy in $\text{Ca}(\text{OH})_2$ medium was of $E_a = 45 \text{ kJ mol}^{-1}$. Thus, the kinetic expression for the progressive conversion period in $\text{Ca}(\text{OH})_2$ medium is the following:

For $[\text{OH}^-] > 3.39 \times 10^{-4} \text{ mol L}^{-1}$:

$$1 - (1 - X)^{1/3} = 7.72 \times 10^6 \cdot e^{-45,000/RT} \cdot [\text{OH}^-]^{0.5} \cdot t \quad (8)$$

Table 1. Decomposition of argentian lead jarosite in Ca(OH)₂ medium: $n = 0.1$, $E_a = 68.56 \text{ kJ mol}^{-1}$ for the induction period; $n = 0.5$, $E_a = 45 \text{ kJ mol}^{-1}$ for the progressive conversion period.

pH	[CaO] (mol L ⁻¹)	[OH ⁻] (mol L ⁻¹)	T (°C)	d ₀ (μm)	θ (min)	k _{exp} (min ⁻¹)
11.90	0.001800	0.007900	22	7 ± 2	246	0.0034
11.80	0.001800	0.006400	26	7 ± 2	41	0.0080
11.60	0.001800	0.005800	30	7 ± 2	57	0.0107
11.43	0.001800	0.005600	35	7 ± 2	29	0.0124
11.19	0.001800	0.004500	40	7 ± 2	18	0.0187
11.04	0.001800	0.004400	45	7 ± 2	10	0.0200
11.23	0.003600	0.009015	50	7 ± 2	12	0.0253
10.95	0.001800	0.004900	50	7 ± 2	12	0.0252
10.91	0.001800	0.005900	55	7 ± 2	10	0.0286
10.54	0.000893	0.001900	50	7 ± 2	34	0.0255
10.06	0.000306	0.000631	50	7 ± 2	10	0.0079
9.79	0.000225	0.000339	50	7 ± 2	22	0.0061

Table 2. Decomposition of argentian lead jarosite in NaOH medium: $n = 1.19$, $E_a = 66.38 \text{ kJ mol}^{-1}$ for the induction period; $n = 0.74$, $E_a = 85.24 \text{ kJ mol}^{-1}$ for the progressive conversion period.

pH	[NaOH] (mol L ⁻¹)	[OH ⁻] (mol L ⁻¹)	T (°C)	d ₀ (μm)	θ (min)	k _{exp} (min ⁻¹)
13.06	0.1070	0.116	25	7 ± 2	4	0.0154
12.97	0.1070	0.113	28	7 ± 2	3	0.0357
12.88	0.1070	0.111	30	7 ± 2	2	0.0582
12.72	0.1070	0.108	35	7 ± 2	1	0.145
12.56	0.1070	0.104	40	7 ± 2	0	0.175
12.40	0.1070	0.0988	45	7 ± 2	0	0.205
12.23	0.1070	0.0903	50	7 ± 2	0	0.28
11.90	0.0709	0.0422	50	7 ± 2	0.5	0.1931
11.80	0.0350	0.035	50	7 ± 2	1.5	0.198
11.72	0.0300	0.0279	50	7 ± 2	4	0.1544
11.30	0.0130	0.0106	50	7 ± 2	6	0.0796
11.10	0.0060	0.00668	50	7 ± 2	7.5	0.0275

Table 3. Cyanidation of argentian lead jarosite in NaOH medium: $n = 0$, $E_a = 167.78 \text{ kJ mol}^{-1}$ for the induction period; $n = 0$, $E_a = 137.38 \text{ kJ mol}^{-1}$ for the progressive conversion period.

pH	[NaOH] (mol L ⁻¹)	[OH ⁻] (mol L ⁻¹)	[CN ⁻] (mol L ⁻¹)	T (°C)	d ₀ (μm)	θ (min)	k _{exp} (min ⁻¹)
13.03	0.1070	0.1080	0.02040	25	7 ± 2	30.100	0.0013
12.88	0.1070	0.1110	0.02040	30	7 ± 2	24.850	0.0106
12.74	0.1070	0.1130	0.02040	35	7 ± 2	20.150	0.0192
12.61	0.1070	0.1170	0.02040	40	7 ± 2	2.000	0.0757
12.47	0.1070	0.1160	0.02040	45	7 ± 2	0.500	0.1230
12.34	0.1070	0.1160	0.02040	50	7 ± 2	0.000	0.4190
12.29	0.1070	0.1030	0.05100	50	7 ± 2	0.000	0.1570
12.31	0.1070	0.1080	0.03600	50	7 ± 2	0.000	0.1750
12.32	0.1070	0.1110	0.00501	50	7 ± 2	0.000	0.1620
12.31	0.1070	0.1080	0.01020	50	7 ± 2	0.000	0.0390

For the progressive conversion period corresponding to the decomposition of the argentian lead jarosite in NaOH media with $[\text{OH}^-] > 6.68 \times 10^{-3} \text{ mol L}^{-1}$, a reaction order of $n = 0.74$ was obtained. The activation energy in NaOH was of $E_a = 85.24 \text{ kJ mol}^{-1}$. Therefore, the kinetic expression for the progressive conversion period in NaOH medium is:

For $[\text{OH}^-] > 6.68 \times 10^{-3} \text{ mol L}^{-1}$:

$$1 - (1 - X)^{1/3} = 1.21 \times 10^{14} \cdot e^{-85.240/RT} \cdot [\text{OH}^-]^{0.74} \cdot t \quad (9)$$

For the case of the argentian lead jarosite cyanidation with $[\text{CN}^-] > 1.02 \times 10^{-2} \text{ mol L}^{-1}$, a reaction order of $n = 0$ was obtained. The activation energy was $E_a = 137.38 \text{ kJ mol}^{-1}$. Thus, the kinetic expression for the cyanidation is the following:

For $[\text{CN}^-] > 1.02 \times 10^{-2} \text{ mol L}^{-1}$:

$$1 - (1 - X)^{1/3} = 2.76 \times 10^{21} \cdot e^{-137.380/RT} \cdot [\text{CN}^-]^0 \cdot t \quad (10)$$

Fig. 6, 7 and 8 represent the model developed with equations 5, 6 and 7; they show the experimental induction period (θ_{exp} min) against the calculated induction period (θ_{calc} min). Since the induction and progressive conversion periods have

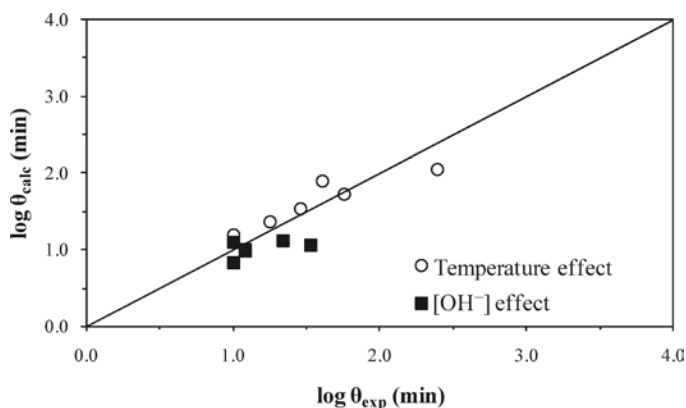


Fig. 6. Induction period. Comparison between calculated and experimental data for θ . $\text{Ca}(\text{OH})_2$ medium, $[\text{OH}^-] > 3.39 \times 10^{-4} \text{ mol L}^{-1}$.

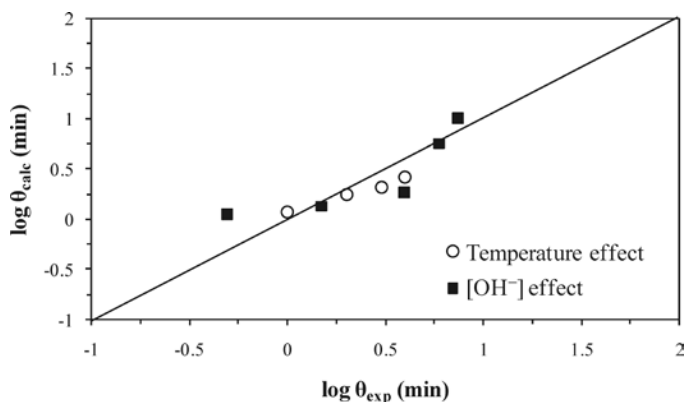


Fig. 7. Induction period. Comparison between calculated and experimental data for θ . NaOH medium, $[\text{OH}^-] > 6.68 \times 10^{-3} \text{ mol L}^{-1}$.

different magnitude orders, their values were plotted in a logarithmic fashion.

Fig. 9 represents the development of equation 8. It outlines the experimental rate constant against the calculated rate constant, i.e. $k_{\text{exp}} (\text{min}^{-1})$ Vs $k_{\text{calc}} (\text{min}^{-1})$ in $\text{Ca}(\text{OH})_2$ medium. In the same way, Fig. 10 describes the development of equation 9, which represents the behavior of the progressive conversion period in NaOH medium. In the case of the cyanidation, Fig. 11 describes the development of equation 10, which corresponds to the behavior of the progressive conversion period in the cyanidation, with a constant concentration of OH ions.

In all of the kinetic expressions $V_M = 169.02 \text{ cm}^3 \text{ mol}^{-1}$, $R = 8.3144 \text{ J mol}^{-1} \text{ K}$, r_0 in cm, T in Kelvin, $[\text{OH}^-]$ in mol L^{-1} , $[\text{CN}^-]$ in mol L^{-1} and t in minutes.

From equations 5 and 8 corresponding to the alkaline decomposition in $\text{Ca}(\text{OH})_2$ medium with $[\text{OH}^-] > 3.39 \times 10^{-4} \text{ mol L}^{-1}$, a general expression can be established to determine the total reaction time necessary to obtain a complete conversion of the argentian lead jarosite. The kinetic model is the following:

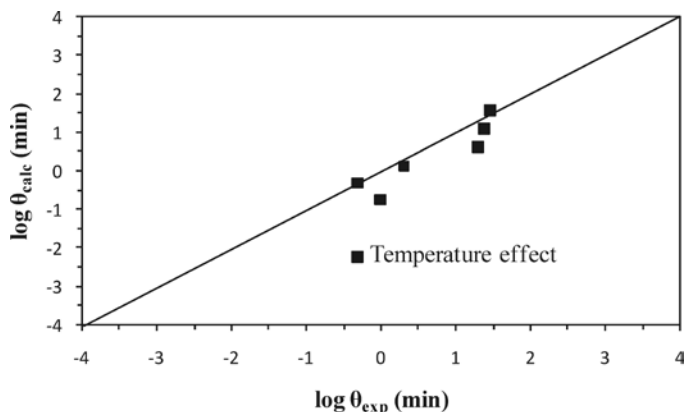


Fig. 8. Induction period for the cyanidation in NaOH medium. Comparison between calculated and experimental data for θ . Complexing NaCN, $[\text{CN}^-] > 1.02 \times 10^{-2} \text{ mol L}^{-1}$.

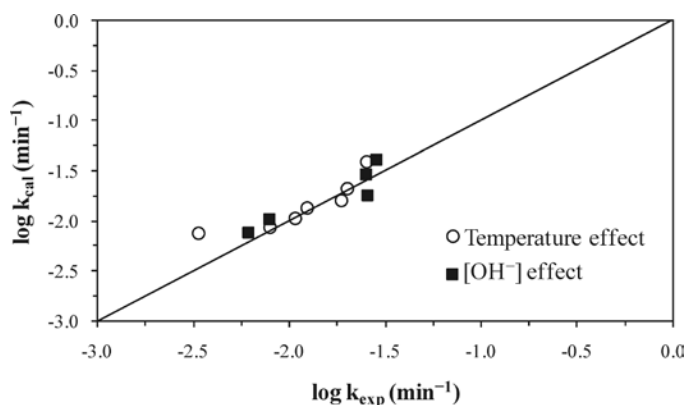


Fig. 9. Progressive conversion period. Comparison between calculated and experimental data for k_{exp} . $\text{Ca}(\text{OH})_2$ medium, $[\text{OH}^-] > 3.39 \times 10^{-4} \text{ mol L}^{-1}$.

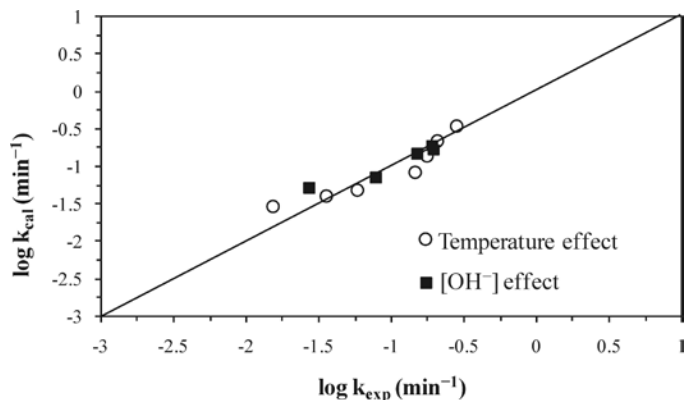


Fig. 10. Progressive conversion period. Comparison between calculated and experimental data for k_{exp} . NaOH medium, $[\text{OH}^-] > 6.68 \times 10^{-3} \text{ mol L}^{-1}$.

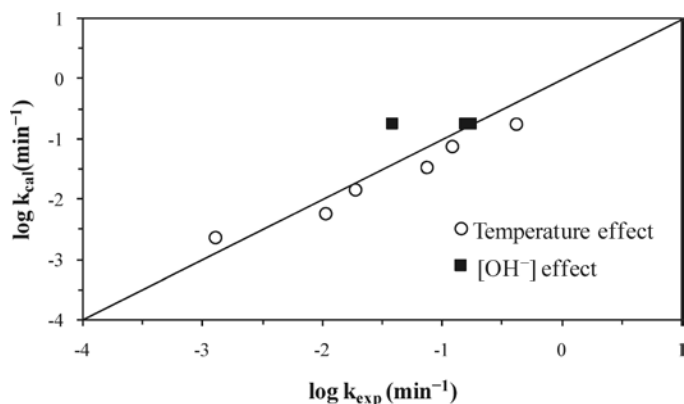


Fig. 11. Progressive conversion period for the cyanidation in NaOH medium. Comparison between calculated and experimental data for k_{exp} . Complexing NaCN, $[\text{CN}^-] > 1.02 \times 10^{-2} \text{ mol L}^{-1}$.

$$t_x = \frac{1}{\left(\frac{1}{r_0 v_M}\right) \cdot [\text{OH}^-]^{0.1} \cdot 1.21 \times 10^9 \cdot e^{-68,568/RT} + \frac{1 - (1 - X)^{1/3}}{7.72 \times 10^6 \cdot e^{-45,000/RT} \cdot [\text{OH}^-]^{0.5}}} \quad (11)$$

Fig. 12 shows the total reaction time necessary to obtain an argentic lead jarosite conversion of $X = 0.75$ (calculated according to equation 11) Vs the same parameter experimentally obtained. It can be concluded that equation 11 is consistent with the experimental results, because they do not differ considerably from the calculated data.

For equations 6 and 9 corresponding to the decomposition in NaOH with $[\text{OH}^-] > 3.39 \times 10^{-4} \text{ mol L}^{-1}$, an expression was established to determine the total reaction time necessary to obtain a complete conversion of argentic lead jarosite. The kinetic model is the following:

$$t_{0.75} = \frac{1}{\left(\frac{1}{r_0 v_M}\right) \cdot [\text{OH}^-]^{1.19} \cdot 1.25 \times 10^{11} \cdot e^{-66,382/RT} + \frac{1 - (1 - X)^{1/3}}{1.21 \times 10^{14} \cdot e^{-85,240/RT} \cdot [\text{OH}^-]^{0.74}}} \quad (12)$$

Fig. 13 shows the total reaction time necessary to obtain a conversion of $X = 0.75$ (calculated according to equation 12) Vs the same parameter (experimentally obtained). It can be concluded that equation 12 is consistent with the experimental results of the decomposition in NaOH medium.

For equations 7 and 10 corresponding to the cyanidation in NaOH medium with $[\text{CN}^-] > 1.02 \times 10^{-2} \text{ mol L}^{-1}$, an expression was established to determine the total reaction time necessary to obtain a complete conversion of argentic lead jarosite. The kinetic model is the following:

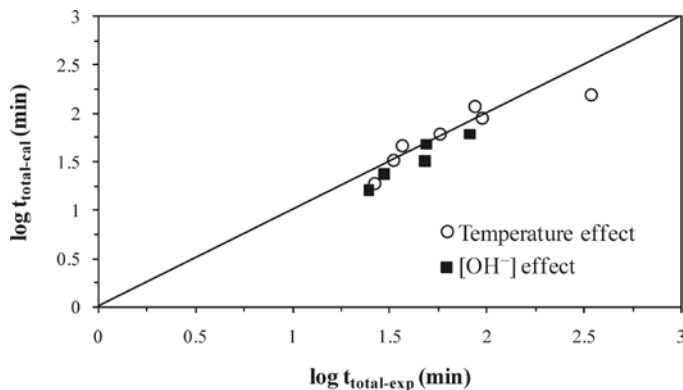


Fig. 12. Alkaline decomposition in $\text{Ca}(\text{OH})_2$ medium. Plot of the total reaction time obtained for a conversion of $X = 0.75$ (experimental and calculated).

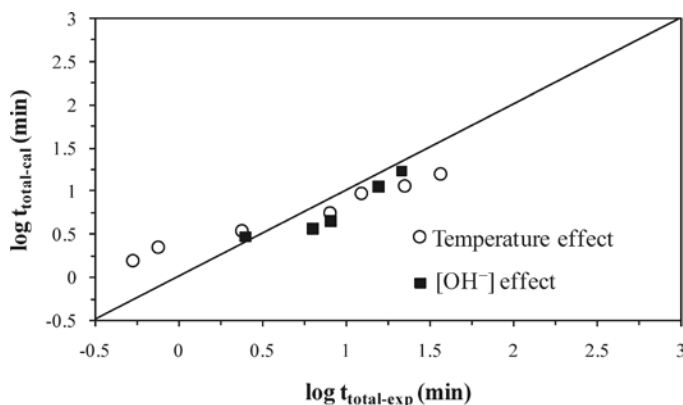


Fig. 13. Decomposition in NaOH medium. Plot of the total reaction time obtained for a conversion of $X = 0.75$ (experimental and calculated).

$$t_x = \frac{1}{\left(\frac{1}{r_0 v_M}\right) \cdot [\text{OH}^-]^0 \cdot 4.22 \times 10^{26} \cdot e^{-167,780/RT}} + \frac{1 - (1 - X)^{1/3}}{2.76 \times 10^{21} \cdot e^{-137,380/RT} \cdot [\text{CN}^-]^0} \quad (13)$$

Fig. 14 shows the total reaction time necessary to obtain a silver dissolution of $X = 0.75$ (calculated according to expression 13) Vs the same parameter (experimentally obtained). According to the obtained data, we can conclude that expression 13 is consistent with the experimental results.

Fig. 15 outlines the calculated induction times Vs the experimental induction times in different media for alkaline decomposition ($\text{Ca}(\text{OH})_2$ and NaOH) and cyanidation in NaOH medium. It confirms that the experimental data are consistent with the kinetic models of equations 5, 6 and 7. Accordingly, Fig. 16 presents the calculated rate constants Vs the experimental rate constants for the progressive conversion period in different media for alkaline decomposition ($\text{Ca}(\text{OH})_2$ and NaOH) and cyanidation (NaCN), confirming that both experimental and calculated data are consistent with the kinetic models of

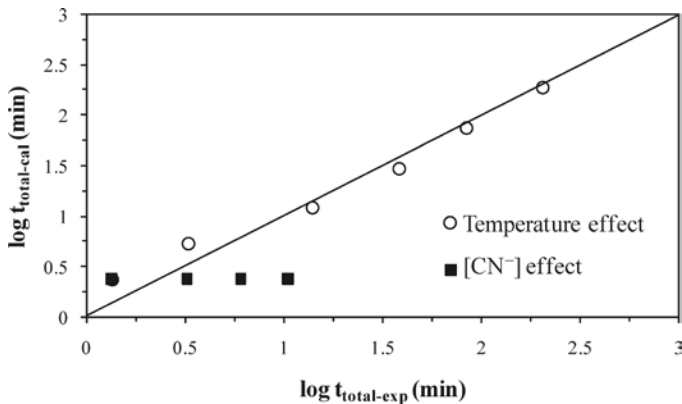


Fig. 14. Cyanidation in NaOH medium. Plot of the total reaction time obtained for a conversion of $X = 0.75$ (experimental and calculated).

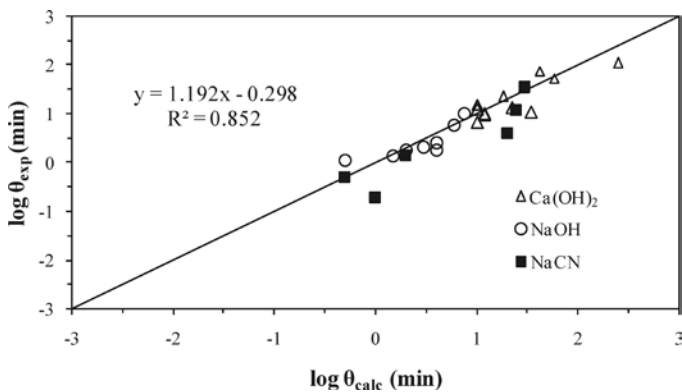


Fig. 15. Global representation of the induction period in different alkaline decomposition media ($\text{Ca}(\text{OH})_2$ and NaOH), as well as cyanidation in NaOH medium.

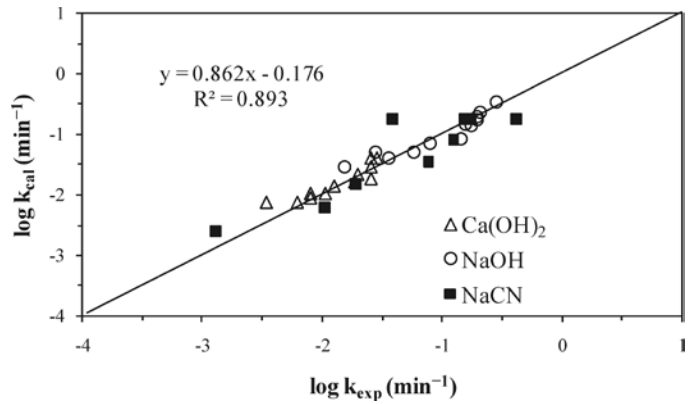


Fig. 16. Global representation of the progressive conversion period in different alkaline decomposition media ($\text{Ca}(\text{OH})_2$ and NaOH), as well as cyanidation in NaOH medium.

equations 8, 9 and 10. In a similar way, Fig. 17 shows the total reaction time necessary to obtain a conversion of $X = 0.75$ in different media for decomposition ($\text{Ca}(\text{OH})_2$ and NaOH) and cyanidation. It confirms that the experimental and calculated data are consistent with the global kinetic models of equations 11, 12 and 13.

Conclusions

The expressions of the global mathematical models for the alkaline decomposition of argentinian lead jarosite regarding the induction period and progressive conversion period in $\text{Ca}(\text{OH})_2$ medium with $[\text{OH}^-] > 3.39 \times 10^{-4} \text{ mol L}^{-1}$ and in NaOH medium with $[\text{OH}^-] > 6.68 \times 10^{-3} \text{ mol L}^{-1}$, as well as for the cyanidation in NaOH medium with $[\text{CN}^-] > 1.02 \times 10^{-2} \text{ mol L}^{-1}$, are the following:

$$t_x = \frac{1}{\left(\frac{1}{r_0 v_M}\right) \cdot [\text{OH}^-]^{0.1} \cdot 1.21 \times 10^9 \cdot e^{-68,568/RT}} + \frac{1 - (1 - X)^{1/3}}{7.72 \times 10^6 \cdot e^{-45,000/RT} \cdot [\text{OH}^-]^{0.5}} \quad (11)$$

$$t_{0.75} = \frac{1}{\left(\frac{1}{r_0 v_M}\right) \cdot [\text{OH}^-]^{1.19} \cdot 1.25 \times 10^{11} \cdot e^{-66,382/RT}} + \frac{1 - (1 - X)^{1/3}}{1.21 \times 10^{14} \cdot e^{-85,240/RT} \cdot [\text{OH}^-]^{0.74}} \quad (12)$$

$$t_x = \frac{1}{\left(\frac{1}{r_0 v_M}\right) \cdot [\text{CN}^-]^0 \cdot 4.22 \times 10^{26} \cdot e^{-167,780/RT}} + \frac{1 - (1 - X)^{1/3}}{2.76 \times 10^{21} \cdot e^{-137,380/RT} \cdot [\text{CN}^-]^0} \quad (13)$$

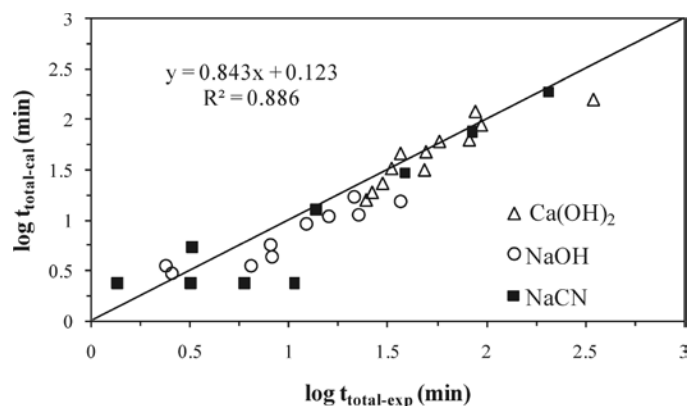


Fig. 17. Global representation of the total reaction time obtained for a conversion of $X = 0.75$ in different alkaline decomposition media ($\text{Ca}(\text{OH})_2$ and NaOH), as well as cyanidation in NaOH medium.

Experimental

Materials

Argentinean lead jarosite with a formula of $(\text{Pb}_{0.32}\text{H}_3\text{O}_{0.35}\text{Ag}_{0.011})\text{Fe}_3(\text{SO}_4)_2(\text{OH})_6$ was used for this study. It was synthesized as described in previous works [3, 21]. The jarosite particles consist of rhombohedral crystal aggregates with a particle size of $7 \mu\text{m}$ and a density of 3170 kg m^{-3} . Fig. 1 is an aggregate particle. Extensive characterization of argentinean lead jarosite can be found in previous works by Patiño *et al.* [3].

Experimental procedure

The used experimental procedure was similar to that of previous works [6, 20]. For the decomposition in NaOH , 0.25 g of argentinean lead jarosite were suspended in a volume of 500 mL. In $\text{Ca}(\text{OH})_2$ media, 0.50 g of argentinean lead jarosite were used in an initial volume of 2 L to prevent CaSO_4 saturation. The same conditions were used for the cyanidation study. OH^- concentration was calculated by taking pH and ionization constant of water at working temperature as a base [22]. As in previous works [7, 10, 20], the progress of the decomposition reaction was followed by sulfur analysis with an Inductively Coupled Plasma (ICP) spectrometer. For the cyanidation, the reaction progress was followed by silver analysis with an Atomic Absorption Spectrophotometer (AAS). Solids obtained at different conversion values were characterized by X-ray Diffraction (XRD), Scanning Electron Microscopy (SEM) and Energy-dispersive X-ray spectroscopy (EDS). Induction time θ , experimental rate constant (k_{exp}), reaction order n and activation energy E_a were determined in all the experiments. With the obtained information, we conducted the kinetic modeling of the alkaline decomposition and cyanidation of the argentinean lead jarosite. Tables 1, 2 and 3 summarize the conditions and the

data obtained experimentally, which were used for the kinetic modeling proposed in this paper.

References

1. Dutrizac, J. E.; Kaiman, S. *Can. Mineral.* **1976**, *14*, 151-158.
2. Smith, A. M. L.; Dubbin, W. E.; Wright, K.; Hudson-Edwards, K. A. *Chem. Geol.* **2006**, *229*, 344-361.
3. Patiño, F.; Ramírez, J. *Rev. Soc. Quím. Méx.* **1993**, *37*, 51-62.
4. Hendricks, S. B. *Am. Mineral.* **1973**, *22*, 773-784.
5. Dutrizac, J. E. *Metall. Trans.* **1983**, *B 14B*, 531-539.
6. Patiño, F. PhD Thesis: "Cinética de la cianuración de argentojarosita y sus soluciones sólidas con plumbojarosita", Universitat de Barcelona, Facultat de Química, España, **1991**.
7. Patiño, F.; Reyes, I.; Rivera I.; Reyes, M.; Hernández, J.; Pérez, M. *J. Mex. Chem. Soc.* **2011**, *55*, 208-213.
8. Patiño, F.; Salinas, E.; Cruells, M.; Roca, A.; *Hydrometallurgy* **1998**, *49*, 323-336.
9. Salinas, E.; Cerecedo, E.; Patiño, F.; Pérez, M. *Metall. Trans.* **2012**, *B H3B*, 1027-1033.
10. Roca, A.; Cruells, M.; Patiño, F.; Rivera, I.; Plata, M. *Hydrometallurgy* **2006**, *81*, 15-23.
11. Cruells, M.; Roca, A.; Patiño, F.; Salinas, E.; Rivera, I. *Hydrometallurgy* **2000**, *55*, 153-163.
12. Patiño, F.; Roca, A.; Reyes, M.; Cruells, M.; Rivera, I. *J. Mex. Chem. Soc.* **2010**, *54*, 216-222.
13. Patiño, F.; Yta, M.; Córdoba, D.A. *Rev. Soc. Quím. Méx.* **1996**, *40*, 61-73.
14. Reyes, I.A.; Patiño, F.; Rivera, I.; Flores, M. U.; Reyes, M.; Hernández, J. *J. Braz. Chem. Soc.* **2011**, *22*, 2260-2267.
15. Flores, M. U.; Patiño, F.; Reyes, I. A.; Rivera, I.; Reyes, M.; Juárez, J. C. *J. Braz. Chem. Soc.* **2012**, *23*, 1018-1023.
16. Russel, C.; Neel, C.; Brill, H. *Sci. Total Environ.* **2000**, *263*, 209-219.
17. Dutrizac, J. E.; Jambor, J. L. Formation and characterization of argentojarosite and plumbojarosite and their relevance to metallurgical processing. In: W.C. Park, D.M. Hausen and R.D. Hagni (Editors); Applied Mineralogy. AIME, Warrendale, Pa. **1984**, 507-530.
18. Dutrizac, J. E. Jarosite-type compounds and their application in the metallurgical industry. In: K. Osseo-Asare and J.D. Miller (Editors), Hydrometallurgy, Research, Development and Plant Practice. TMS-AIME, Warrendale, Pa. **1982**, 531-551.
19. Dutrizac, J. E.; Jambor, J. L. *Trans. Inst. Min. Metall.*, **1987**, *C 96C*, 206-218.
20. Patiño, F.; Viñals, J.; Roca, A.; Núñez, C. *Hydrometallurgy* **1994**, *34*, 279-291.
21. Canales, J. J. PhD Thesis: "Síntesis, descomposición y cianuración de la jarosita de plomo argentífera en medio NaOH ", Universidad Autónoma del Estado de Hidalgo, A.A.C.T. y M., México, **2009**.
22. Lide, D. R. *Handbook of chemistry and physics*, Eds. CRC Press, Boston, **2009**, 8-79.
23. Patiño, F.; Cruells, M.; Roca, A.; Salinas, E.; Pérez, M. *Hydrometallurgy* **2003**, *70*, 153-161.
24. Sohn, H. Y.; Wadsworth, M. E. *Cinética de los procesos de la Metalurgia Extractiva*, Ed. Trillas, México, **1986**, 167-194.
25. Ballester, A.; Verdeja, L. F.; Sancho, J. *Metalurgia Extractiva*, Vol. 1. Fundamentos, Editorial Síntesis, Madrid, **2000**, 182-189.
26. Levenspiel, O. *Ingeniería de las Reacciones Químicas*, Editorial Reverté, España, **2005**, 393-448.